ASISH MALAS, CHAPAL KUMAR DAS[*)]

Indian Institute of Technology
Materials Science Centre
Kharagpur — 721302, India

Compatibilized ethylene-propylene-diene terpolymer nanocomposites containing different type of organoclays

Summary — The simple mixing of non-polar rubber and organically modified nanoclay may not lead to good dispersion of organoclay in the rubber matrix, which is due to the incompatibility between the rubber and the filler. Thus, the application of polar compatibilizer which is compatible with both the gum base and organically modified clay may help to increase the reinforcing efficiency of the organoclay. Oil extended carboxylated styrene-butadiene rubber (XSBR) was used as a compatibilizer for the dispersion of the organically modified clay (Cloisite 15A, Cloisite 20A and Cloisite 30B) in the ethylene-propylene-diene terpolymer (EPDM) matrix. The degree of dispersion of organoclays in non-polar EPDM matrix after application of polar compatibilizer as well as the influence of these organoclays on the properties of nanocomposites based on EPDM were analyzed in this study. The microstructure of the organoclay filled EPDM composites was studied by wide angle X-ray diffraction (WAXD) method and high resolution transmission electron microscopic (HR-TEM) analysis. Dynamic mechanical thermal analysis (DMTA), scanning electron microscopic (SEM) analysis, thermogravimetric analysis (TGA) and curing tests were conducted for each nanocomposite. Cloisite 30B filled EPDM composite showed best thermal, mechanical and dynamic mechanical properties compared to all other investigated nanocomposites.
Keywords: blend, clay, compatibility, compounding, crosslinking.

KOMPATYBILIZOWANE NANOKOMPOZYTY TERPOLIMERU ETYLENOWO-PROPYLENO-WO-DIENOWEGO ZAWIERAJĄCE RÓŻNE RODZAJE ORGANICZNIE MODYFIKOWANYCH GLINEK
Streszczenie — Proste mieszanie niepolarnej gumy i polarnej organicznie zmodyfikowanej nanoglinki może nie wystarczyć do dobrego rozproszenia tej glinki w matrycy kauczuku. Jest to spowodowane brakiem kompatybilności między gumą i wypełniaczem. Zastosowanie polarnego kompatybilizatora, który jest kompatybilny z gumą bazową jak i z polarną organicznie modyfikowaną glinką, może pomóc w zwiększeniu efektywności wbudowywania w matryce gumowe organiczne modyfikowanych glinek. W tej pracy do wbudowania organicznie modyfikowanych nanoglinek (Cloisite 15A, Cloisite 20A i Cloisite 30B) w matrycę niepolarnego terpolimeru etylenowo-propylenowo-dienowego (EPDM) użyto modyfikowanego olejem polarnego karboksylowanego kauczuku butadienowo-styrenowego (XSBR). Zbadano stopień dyspersji nanoglinki w matrycy niepolarnego EPDM po zastosowaniu polarnego kompatybilizatora oraz wpływ rodzaju glinki z kompatybilizatorem na właściwości otrzymanych nanokompozytów na bazie EPDM. Wszystkie nanokompozyty badano metodami szerokokątowej dyfrakcji promieniowania rentgenowskiego (WAXD), wysokorozdzielczej transmisyjnej mikroskopii elektronowej (HR-TEM), dynamicznej analizy termomechanicznej (DMTA), skaningowej mikroskopii elektronowej (SEM) oraz analizy termograwimetrycznej (TGA). Kompozyt EPDM napełniony Cloisite 30B charakteryzował się najlepszymi właściwościami termicznymi, mechanicznymi i dynamicznymi spośród wszystkich badanych nanokompozytów.
Słowa kluczowe: mieszanka, glinka, kompatybilność, mieszanie składników, sieciowanie.

INTRODUCTION

The main target in preparing organoclay nanocomposites is to achieve a better degree of dispersion of orga-

---
[*)] Corresponding author; e-mail: chapal12@yahoo.co.in

noclay aggregates in the polymer matrices, which can yield to very large surface area. This in turn remarkably improves the overall properties of the nanocomposites. The majority of the works have been done in clay filled nanocomposites for many thermoplastics and thermosetting polymers. But the studies on rubber based nanocomposites constitute in lesser dimension [1—4]. Properly dispersed nanofiller, having high aspect ratio and stiffness in the polymer matrices could lead to increase in the mechanical properties of the nanocomposites compared to the properties of neat polymer. As most of the nanofillers are inorganic in nature so it is difficult to disperse them in the organic polymer matrices. Montmorillonite (MMT) is the most widely used layered silicates due to its natural occurrence and some outstanding properties such as high cation exchange capacity, high surface area and also high aspect ratio [2]. As layered silicates are hydrophilic in nature so in order to improve their dispersion in the polymer matrices, modifications of these fillers by organic surfactants and addition of compatibilizer are required. To modify the hydrophilic layered silicates to organophilic, their cation exchange capacity is employed. The modified layered silicates are known as organoclays. Organoclays are generally prepared by exchanging the alkali cations with alkyl ammonium ions [5—7]. The modification of layered silicates causes a change in the surface polarity of the clay and widens the intergallery space of the layered silicates. The reinforcing efficiency of the organoclays in the polymer matrices is very high due to their nanometer phase dimensions, which indeed create a very large surface area.

The main aim during the preparation of polymer/clay nanocomposites (PCNs) is to disperse the polar organoclays in the different nonpolar polymer matrices properly. PCNs have gained much attention, due to the achievement of desired improvements in the physical, mechanical, thermal, flame retardant, barrier and decreased moisture absorption properties compared to their micro-, macrocomposites and their pure polymer matrices, at very low level loading, in the industrial as well as in the research area [1, 8—15]. The achivement of better dispersion of organically modified clay in the elastomer matrices involves two main faces. The first aspect is the compatibility between the rubber and nanoclay. The organically modified clay is polar, that is why it is not compatible with the non polar rubbers like ethylene-propylene-diene terpolymer (EPDM), styrene-butadiene rubber (SBR), *etc*. For the sake of compatibility, oil extended carboxylated styrene-butadiene rubber (XSBR), epoxidized natural rubber (ENR), *etc*., which are quite polar and compatible with the organically modified clays as well as with the non polar rubber matrices can be used. A few good works have been carried out using epoxidized natural rubber as a compatibilizer by Arroyo *et al*. [16], Teh *et al*. [17] and Varghese *et al*. [18]. Also in our laboratory we have studied the effect of organoclay in some rubber matrices like natural rubber (NR) [19, 20], SBR [21] and nitrile-buta-

diene rubber (NBR) [22] by using epoxidized natural rubber as a compatibilizer.

The second aspect is the method used for the production of nanocomposites. There are mainly four different procedures generally used like for the nanocomposites preparation *in-situ* polymerization intercalation [23], solution intercalation [24], melt intercalation [17] and finally coagulation of rubber latex and clay aqueous suspension [25] for the preparation of PCNs.

In the present work we have used three different types of organically modified clay as nanofiller and XSBR as a compatibilizer between polar nanoclay and the non-polar EPDM. Firstly in order to get uniform dispersion of organoclay in the XSBR matrix each organoclay was incorporated in XSBR separately by solution mixing method. After that the XSBR-nanoclay (XC) composites were incorporated in the base EPDM matrix with sulphur as a curing agent using a laboratory scale two roll mixing mill. The changes obtained in the morphology, curing characteristics, mechanical properties, dynamic mechanical properties and thermal stability of the different nanocomposites were extensively studied and compared with each other and also with the neat EPDM compound.

EXPERIMENTAL

Materials

To prepare nanocomposites ethylene-propylene-diene copolymer (EPDM) was used. EPDM under the trade name Royalene 535 (Netherlands) characterized by (ethylene/propylene weight ratio 60/40, and ethylidene nonbornene content (ENB) 9.4 wt. % was purchased from DSM Elastomer B. V.

Oil extended carboxylated styrene butadiene rubber (1.6 mol. % methacrylic acid) was obtained from Lanxess India Pvt. Ltd.

Organically modified clays (Cloisite 15A, Cloisite 20A and Cloisite 30B) were supplied from Southern Clay Products, Inc. (USA). These are organically modified montmorillonites with literature lateral dimensions of 100 nm to more than 1000 nm [26]. For Cloisite 30B (modifier concentration: 90 meq/100 g of clay), the organic modifier is methyl tallowyl bis-2-hydroxy ethyl ammonium chloride (quaternary salt MT 2 EtOH). For both Cloisite 15A (modifier concentration: 125 meq/100 g clay) and Cloisite 20A (modifier concentration: 95 meq/100 g clay), the organic modifier is dimethyl dihydrogenated tallowyl ammonium chloride (quaternary salt, 2M2HT). The structure of the surfactant of Cloisite 30B, Cloisite 15A and Cloisite 20A are shown below as formulas (I) and (II), respectively [27, 28].

The organic surfactant MT2EtOH residing at the surface of the Cloisite 30B has polar groups but the organic surfactant 2M2HT residing at the surface of the Cloisite 15A and 20A has no polar group, so Cloisite 30B is more polar than the other two organoclays.

HO

Cl$^{\ominus}$

N$^{\oplus}$

HO

(I)

Cl$^{\ominus}$

N$^{\oplus}$

(II)
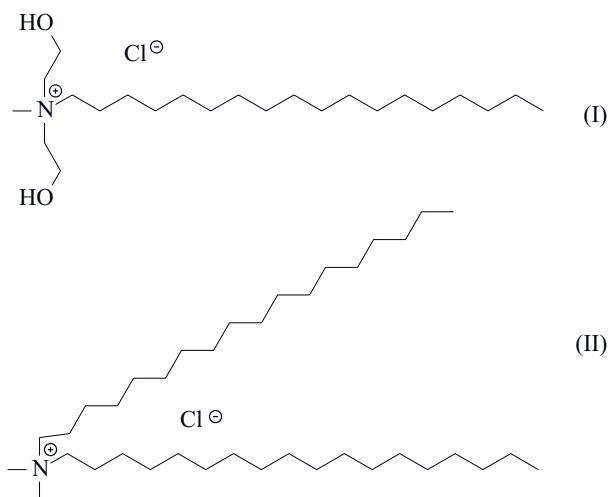
Other compounding additives like sulphur, zinc oxide, stearic acid, *N*-cyclohexyl-2-benzothiazyl sulphenamide (CBS), tetramethylthiuram disulphide (TMTD) were purchased from Bayer (M) Sdn Bhd Malaysia.

Preparation of nanocomposites

In order to improve the dispersion and compatibility of the organoclays with the rubber matrix, solution mixing method was used for the preparation of the XSBR/organoclay composites (XC). At first XSBR was dissolved in toluene (rubber to solvent mass/volume ratio was 1:3 g/cm^3). Then the solution was stirred vigorously (600 rpm) and continuously at room temperature until the compatibilizer (XSBR) completely dissolved in the solvent. After that 50 phr of organoclay was added to the solution under continuous stirring. After some time the whole solution was sonicated for 30 min. Then it was poured into a Petri dish and left in the open air for the total evaporation of the solvent so as to obtain transparent film. Three different compatibilizer/organoclay composites were prepared XSBR/Cloisite 15A (XC1), XSBR/Cloisite 20A (XC2) and XSBR/Cloisite 30B (XC3) by using three different organically modified clays at the same time in three batches.

T a b l e 1. Formulation of the rubber composites

Ingre-dients	Sample symbol			
	EPDM	EPDM/XC1	EPDM/XC2	EPDM/XC3
	Content (phr)			
EPDM	100	94	94	94
XC	—	6	6	6
Stearic acid	1	1	1	1
CBS	1	1	1	1
TMTD	0.5	0.5	0.5	0.5
Zinc oxide	3	3	3	3
Sulphur	1.5	1.5	1.5	1.5

Formulation of the prepared nanocomposites is depicted in Table 1. In XC composites, the amount of orga-

noclay is 50 phr (with respect to XSBR), so in 6 phr of XC composites (with respect to EPDM rubber), the content of organoclay is about 3 phr. The compounding of EPDM rubber was done in an open two roll mixing mill at room temperature and the speed ratio of the rotor was 1:1.4 (front to back). Compression molding machine was used for the vulcanization of the rubber compounds at 150 °C and the optimum cure time was obtained from the rheometer.

Methods of testing

Curing study of the nanocomposites was done at 150 °C with 3° arc for 60 min using Monsanto Rheometer R-100 testing instrument.

Wide angle X-ray diffraction **(**WAXD) analysis of rubber compounds were carried out using a Rigaku Miniflex Diffractometer with Cu-Kα radiation at a generator voltage of 40 kV, a scanning rate 1°/min between 1°—15°, chart speed of 10 mm/2θ, current 20 mA and wavelength of 0.154 nm at room temperature. The *d*-spacing of the nanoclay were obtained from the Brag's equations (nλ = 2d sin θ).

The morphology of the dispersed nanoclay in the solvent casted sample and the three different nanocomposites was observed in high resolution transmission electron microscope (HR-TEM) type JEOL 2100. For HR-TEM analysis, ultra thin cross sections of the specimen were cut using Leica Ultra Cut UCT Ultra microtome instrument equipped with a diamond knife.

Dynamic mechanical thermal analysis (DMTA) of the prepared nanocomposites were done using a thermal analysis instrument DMA 2980 model in tension mode at a constant frequency 1 Hz, a strain of 0.1 %, in a temperature range from -80 °C to +80 °C, at a heating rate of 3 °C/min. The storage moduli (*E'*), loss factor (tan δ) of the different nanocomposites were observed, also the glass-rubber transition temperature (T_g) were obtained from the tan δ plot.

Mechanical properties of the nanocomposites were obtained using universal tensile testing machine Hounsfield H 10KS under ambient conditions (at 25±2 °C) according to ASTM D638 standard. For each set 5 samples were tested and the presented results correspond to the average values. The tensile stress, modulus and elongation at break were obtained at room temperature. The measured length was 25 mm, and the speed of jaw separation was 500 mm/min.

Scanning electron microscopy (SEM) analysis of the tensile fractured surface of the nanocomposites was carried out in VEGA TESCAN// LSU instrument after the fractured surface of the samples were gold coated.

Thermogravimetric analysis (TGA) of the nanocomposites was done using a DuPont TGA- 2100 thermal analyzer in the temperature range from 34 °C to 650 °C with a heating rate of 10 °C/min.

RESULTS AND DISCUSSION

Thermogravimetric analysis

Thermal analysis of the three different organoclay based nanocomposites and the EPDM itself was done by thermogravimetric analyzer in the temperature range 50—650 °C. TGA curves for EPDM/XC1, EPDM/XC2, EPDM/XC3 and neat EPDM are shown in Figure 1. In general, we can see that addition of nanoclay into the polymer matrices increases the thermal stability of the nanocomposites. This may be due to the heat shielding effect of the incorporated nanoclay in the polymer matrix. Futhermore a mass transport barrier to the volatile pro-
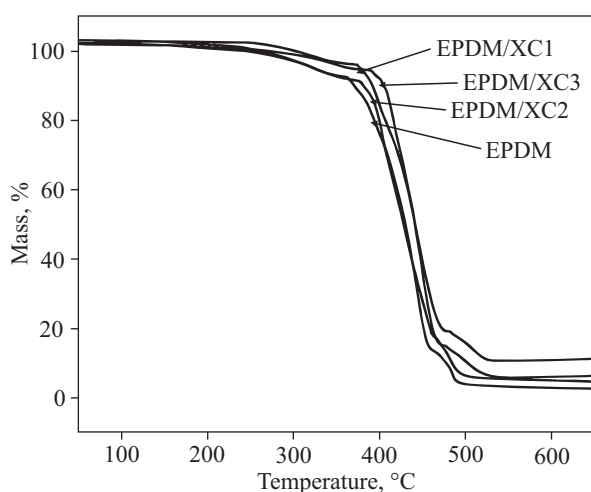
Fig. 1. TGA curves of EPDM nanocomposites containing different nanoclays

Fig. 2. HR-TEM images of composite: a) XC1, b) XC2, c) XC3

ducts produced during decomposition of the nanocomposites may be formed. In this case EPDM/XC3 (Cloisite 30B containing) compound shows comparatively better thermal stability among the three different organoclay based nanocomposites. It can be explained by the better dispersion of the Cloisite 30B nanoclay in the XSBR matrix compared to the other two organoclays. Molecule of the surfactant of Cloisite 30B nanoclay contains two hydroxyl groups so this substance is more polar than the other two organoclays. Cloisite 30B is more compatible with the polar XSBR matrix compared to the other two organoclays as well as it was finely dispersed in the bulk rubber matrix. Also some hydrogen bonds (noncovalent interactions) between the organic modifier of Cloisite 30B and the carboxylic acid groups of XSBR can be formed.

HR-TEM analysis

HR-TEM images for XC1, XC2 and XC3 composites are shown in the Figure 2. Platelets of nanoclay can be seen from the images. Layered silicates were identified by the dark lines in the images. HR-TEM images prove

that the nanoclay platelets were intercalated as well as delaminated in the XSBR matrix. HR-TEM image of XC3 nanocomposite shows better dispersion of Cloisite 30B organoclay platelets in the XSBR matrix as it is more polar compared to the other two organoclays used in the study. Figure 3 shows the HR-TEM images of EPDM/XC1, EPDM/XC2 and EPDM/XC3 nanocomposites, respectively. From all the images it can be seen that some of the nanoclay platelets are partially exfoliated and few are agglomerated in the bulk EPDM matrix.

WAXD analysis

The X-ray diffraction (XRD) pattern of the different organoclays, compatibilizer/organoclay composites and the nanocomposites are depicted in the three different sets in Figure 4. The 2θ values and the corresponding *d*-spacing of each material were tabulated in Table 2. Fig. 4a shows the XRD pattern for Cloisite 15A, XC1 and EPDM/XC1 in the diffraction angle range $1—10°$. As it can be seen in the Fig. 4a, there is an intense peak around $2\theta = 2.71°$, corresponding to the basal spacing 3.32 nm (d_{001}) for Cloisite 15A. For XC1, the main peak (d_{001}) of the Cloisite 15A has been shifted towards the lower angle,
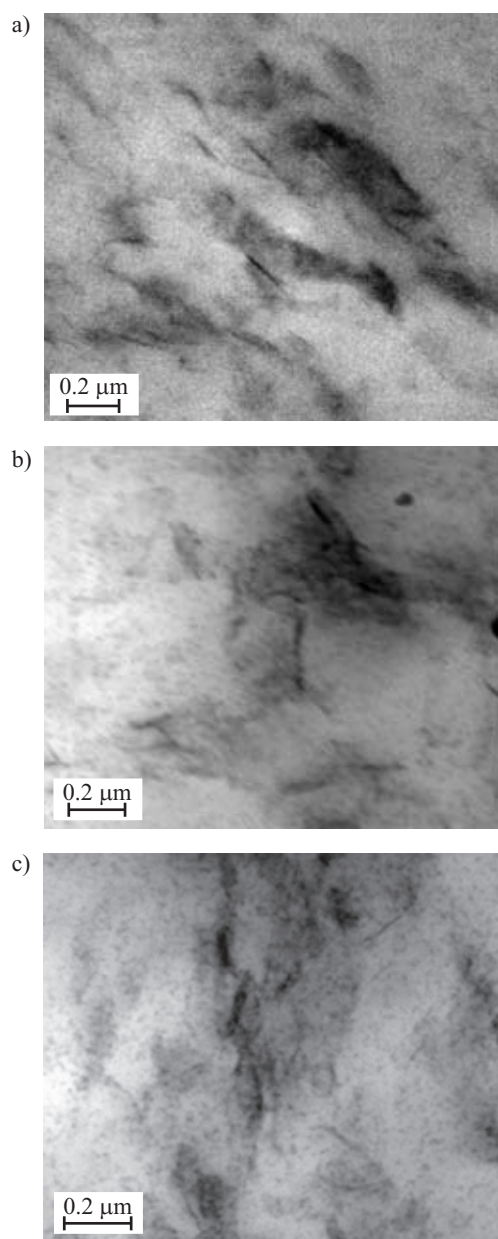
Fig. 3. HR-TEM images of composite: a) EPDM/XC1, b) EPDM/XC2, c) EPDM/XC3

which indicates the presence of intercalated structure [29]. Furthermore along with the primary peak two secondary peaks arise, which may be due to the reaggregation of nanoclay in the XSBR matrix. Strong van der

T a b l e 2. 2θ and the corresponding *d*-spacing values of the different components of nanocomposites

Sample name	2θ, °	*d*-spacing, nm
Cloisite 15A	2.71	3.32 (d_{001})
Cloisite 20A	3.14	2.82 (d_{001})
Cloisite 30B	5.04	1.76 (d_{001})
XC1	1.71, 3.94, 6.13	5.19 (d_{001}), 2.24 (d_{002}), 1.44 (d_{003})
XC2	1.81, 4.08, 6.36	4.92 (d_{001}), 2.14 (d_{002}), 1.40 (d_{003})
XC3	4.78	1.83 (d_{001})
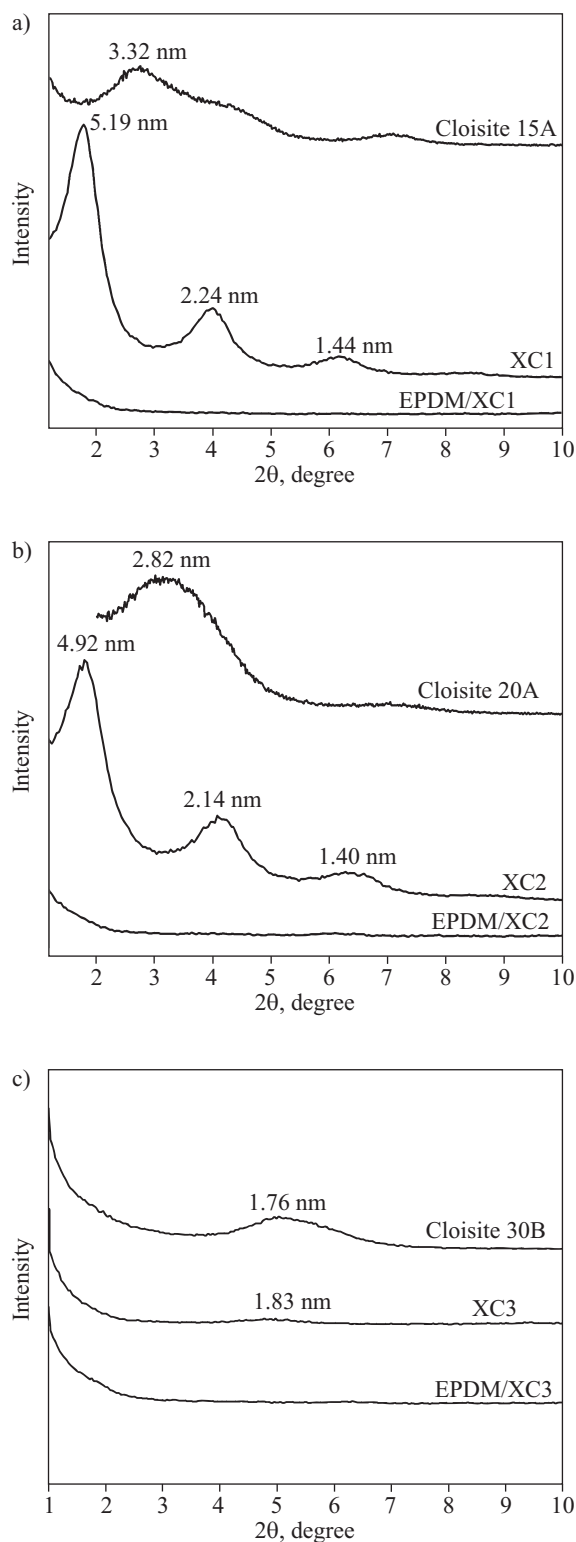
Fig. 4. XRD patterns of: a) Cloisite 15A, XC1 and EPDM/XC1, b) Cloisite 20A, XC2 and EPDM/XC2, c) Cloisite 30B, XC3 and EPDM/XC3

Waals force of interaction among thousands of organoclay platelets resulte in the reaggregation of organoclays in the rubber matrix. For EPDM/XC1 composite, no such peak, were observed which indicates that the nanoclay is partially exfoliated in the EPDM matrix. Similar type of observation has reported by Acharya *et al.* [30] and Das

et al. [31] for the nanocomposites of layered double hydroxide (LDH) with EPDM and polyurethane, respectively. For XC2 and EPDM/XC2 composites, the similar kind of XRD patterns like for XC1 and EPDM/XC1 (Fig. 4b) was observed. The main peak of the Cloisite 20A has been shifted towards the lower angle $2\theta = 1.81°$, corresponding to the basal spacing 4.92 nm (d_{001}) which proves the presence of intercalated structure of XC2 composites. The secondary peaks were diminished relatively to the main peak which also affirms the presence of the intercalated structure [32]. For EPDM/XC2 nanocomposite no such peak was observed which indicates the partial exfoliation of the nanoclay in the bulk EPDM matrix. The main peak of the Cloisite 30B in the XC3 has been shifted towards the lower angle $2\theta = 4.78°$ and intensity of the peak was significantly diminished which indicates the presence of the intercalated structure. Also in this case the nanoclay may be partially exfoliated in the XSBR matrix. This is due to better dispersion of Cloisite 30B nanoclay in the XSBR matrix. For EPDM/XC3 nanocomposite no such peak was observed which indicates the partial exfoliation of the nanoclay in the EPDM matrix.

XRD give patterns only the incomplete evidence of the dispersion of nanofiller. Lack of peak corresponding to *d*-spacing does not always signify the delamination of filler in polymer matrix, because XRD is unable to ascertain regular stacking exceeding 8.8 nm [33]. Therefore, microscopic investigation is necessary to study the morphology of the nanocomposites.

DMTA analysis

The temperature dependence of dynamic storage modulus (*E'*) and loss factor (tan δ) are represented in Fig. 5. The different clay loaded nanocomposites show dramatic increase in *E'* compared to the storage modulus of EPDM. Cloisite 30B, Cloisite 15A and Cloisite 20A loaded EPDM compounds show 88 %, 52 % and 42 %, increase in *E'* at 25 °C, respectively, in comparison with the neat EPDM. EPDM/XC3 shows higher storage modulus compared to the other two nanoclay loaded nanocomposites. Because of highest polarity of Cloisite 30B nanoclay among the three organoclays, it is more compatible with the compatibilizer XSBR as well as it was more finely dispersed into the EPDM matrix.

But it was shown from Fig. 5b that the tan δ peak height was decreased only for the nanocomposite EPDM/XC3 containing Cloisite 30B. EPDM/XC3 exhibits lesser damping characteristics than the other two different nanocomposites. This may be due to better reinforcing effect of Cloisite 30B nanoclay in the EPDM matrix than other two organoclays. Decrease in the tan δ peak height during the dynamic mechanical deformation is due to the restriction in the chain mobility because of physical and chemical adsorption of rubber molecules on the filler surface [34]. Glass-rubber transition temperature (*T_g*) values of the clay loaded nanocomposites were
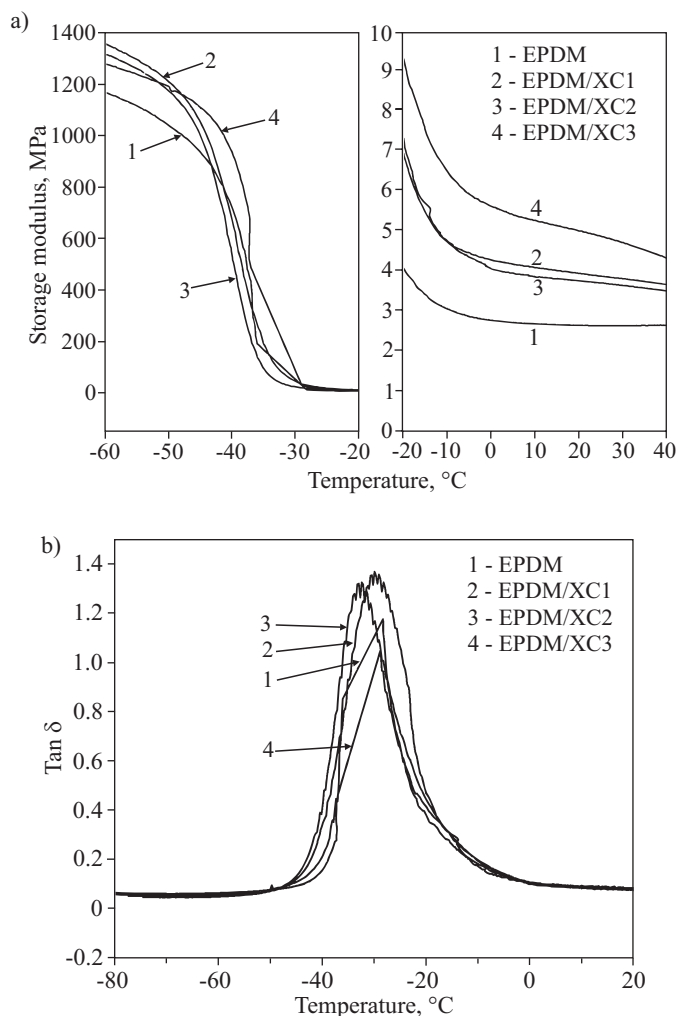
Fig. 5. Storage modulus (a) and tan δ (b) curves of neat EPDM, EPDM/XC1, EPDM/XC2 and EPDM/XC3

decreased compared to the neat EPDM. This is because of the plasticizing effect of the organic surfactant [35, 36] or extra volume was created by the organic surfactant at the polymer silicate interface [37, 38].

Curing characteristics

The curing characteristics of the nanocomposites are depicted in the Table 3. The minimum torque value was increased for all EPDM/XC samples in comparison with neat EPDM as a control sample. The minimum torque value can be considered as a measure of viscosity of the nanocomposites. Maximum of torque can be regarded as a measure of stock modulus or composites modulus [17]. The nanoclay loaded EPDM compounds show improvement in maximum torque value. The improvement in the maximum torque value was highest for the nanocomposites containing Cloisite 30B clay. This may be due to better dispersion of Cloisite 30B clay in the XSBR matrix (compatibilizer) as well as to its finer distribution in the EPDM matrix. Nanoclay loaded EPDM composites show reduced scorch and curing time compared to the neat

T a b l e 3. Curing characteristics of prepared nanocomposites

Sample symbol	Minimal torque dN·m	Maximal torque dN·m	Torque difference, dN·m	Scorch time min	Curing time min	Curing rate index
EPDM	19.0	60.0	41.0	3.48	10	14.25
EPDM/XC1	24.4	64.9	40.5	1.48	8.95	12.88
EPDM/XC2	21.1	61.2	40.1	1.68	6.08	21.43
EPDM/XC3	24.5	65.5	41.0	1.43	8.38	14.02

EPDM. The smaller particle size of the nanoclay platelets having very large surface area promotes the curing reaction and also the onium ions of organoclay behaves as a catalyst, accelerating the vulcanization reaction [1, 3, 17, 24]. The acceleration of the curing reaction by addition of organically modified clays is principally attributed to the presence of onium ions modifier embedded into the clay galleries. The onium ions activates the functional groups of the accelerants, for instance benzothiazyl sulphenamide and thiuram disulphide, giving rise to a synergistic effect that leads to a faster and more effective vulcanization reaction. The nanocomposites containing Cloisite 30B shows faster scorch and cure time than the other two nanocomposites.

Mechanical properties

The mechanical properties of the nanoclay loaded compounds are listed in Table 4. Addition of nanoclay to EPDM improves the mechanical properties of material. Better properties were achieved for Cloisite 30B clay loaded nanocomposites. This may be a result of better dis-

T a b l e 4. Mechanical properties of the prepared nanocomposites

Sample symbol	Tensile strength MPa	Elonga- tion at break, %	100 % modulus MPa	300 % modulus MPa	Tear strength N/mm
EPDM	3.55	401.5	1.46	2.41	9.91
EPDM/XC1	5.26	382.0	1.78	4.59	10.54
EPDM/XC2	4.10	341.2	1.53	3.45	12.08
EPDM/XC3	6.00	302.8	1.54	3.95	12.93

persion Cloisite 30B nanoclay platelets in the XSBR matrix as well as in EPDM matrix due to its higher polarity compared to the other two organoclays. The tensile strength was increased by 69 %, 49 % and 16 % for EPDM/XC3, EPDM/XC1 and EPDM/XC2, respectively, over the neat EPDM. Cloisite 15A nanoclay loaded nanocomposite shows the highest modulus compared to the modulus of the other two nanocomposites, this may be due to its highest d-spacing of that organoclay compared to the other two organoclay which leads to the improved
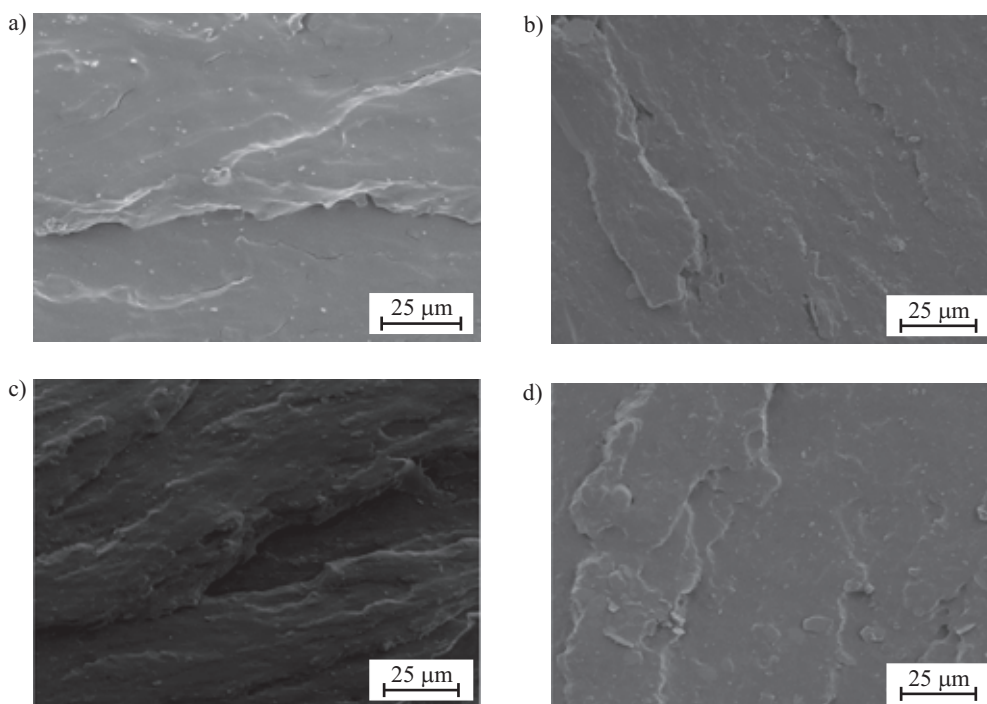
Fig. 6. SEM photographs of: a) neat EPDM, b) EPDM/XC1, c) EPDM/XC2, d) EPDM/XC3

inter-gallery spacing when incorporated in the rubber matrix. The elongation at break is the smallest and tear strength is the highest for the Cloisite 30B nanoclay loaded compound, which may be due to the same reason explained earlier.

SEM analysis

The SEM images of the tensile fractured surface of the organoclay loaded EPDM composites are shown in the Figure 6. Different organoclay loaded EPDM composites show highly rougher surface morphology compared to the neat EPDM. The dispersion of nanoclay platelets in the elastomer matrix alters the crack path depending on their orientation in the EPDM matrix.

CONCLUSIONS

The effect of different organically modified clay on the properties of EPDM has been summarized. The morphology observed from the XRD results and HR-TEM images demonstrates the intercalation, aggregation and partial exfoliation of the nanoclay in the XSBR matrix. Incorporation of XSBR-nanoclay composites into the EPDM matrix leads to exfoliation of the nanoclay. Reduced scorch, curing time and increase in maximum of torque have been observed for the EPDM rubber containing XSBR-nanoclay composites compared to the neat EPDM. Closite 30B organoclay loaded compound showed better curing characteristics, mechanical, thermal and dynamic mechanical thermal properties compared to the other two nanocomposites because of its better dispersion in the EPDM matrix, and more polar nature of this organic surfactant than the other two modified nanoclays.

REFERENCES

1. Arroyo M., Lopez Manchado M. A., Herrero B.: *Polymer* 2003, **44**, 2447.
2. Chang Y., Yang Y., Ryu S., Nah C.: *Polym. Int*. 2002, **51**, 319.
3. Usuki A., Tukigase A., Kato M.: *Polymer* 2002, **43**, 2185.
4. Duquesne S., Jama C., Le Bras M., Delobel R., Recourt P., Gloaguen J. M.: *Compos. Sci. Technol.* 2003, **63**, 1141.
5. Li J. X., Wu J., Chan C. M.: *Polymer* 2000, **41**, 6935.
6. Wang S., Hu Y., Wang Z., Yong T., Chen Z., Fan W.: *Polym. Degrad. Stabil*. 2003, **80**, 157.
7. Giannelis E. P.: *Adv. Mater*. 1996, **8**, 29.
8. Alexandre M., Dubois P.: *Mater. Sci. Eng*. 2000, **28**, 1.
9. Giannelis E. P., Krishnamoorti R., Manias E.: *Adv. Polym. Sci*. 1999, **138**, 107.
10. Pinnavaia T. J., Beall G. W.: „Polymer-clay nanocomposites", John Wiley & Son, New York, 2000.
11. Ray S. S., Okamoto M.: *Prog. Polym. Sci*. 2003, **28**, 1539.
12. Karger-Kocsis J., Wu C. M.: *Polym. Eng. Sci*. 2004, **44**, 1083.
13. Zeng C., Han X., Lee L. J., Koelling K. W., Tomasko D. L.: *Adv. Mater*. 2003, **15**, 1743.
14. Shah D., Maiti P., Jiang D. D., Batt C.A., Giannelis E. P.: *Adv. Mater*. 2005, **17**, 525.
15. Tasai T. Y., Li C. H., Chang C. H., Cheng W. H., Hwang C. L., Wu R. J.: *Adv. Mater*. 2005, **17,** 1769.
16. Arroyo M., Lopez-Manchado M. A., Valentin J. L., Carretero J.: *Compos. Sci. Technol*. 2007, **67**, 1330.
17. Teh P. L., Mohd Ishak Z. A., Hashim A. S., Karger-Kocsis J.: *Eur. Polym. J*. 2004, **40**, 2513.
18. Varghese S., Karger-Kocsis J., Gatos K. G.: *Polymer* 2003**, 44**, 3977.
19. Rajasekar R., Das T., Pal K., Das C. K.: *Nano Trends*: *J. Nanotechnol. Applic*. 2007, **3**, 1.
20. Rajasekar R., Pal K., Pal S. K., Das C. K.: *ICFAI J. Sci. Technol*. 2008, **4**, 17.
21. Rajasekar R., Heinrich G., Das A., Das C. K.: *Res. Lett. Nanotechnol*. 2009, Article ID 405153, doi:10.1155/2009/405153, 1.
22. Rajasekar R., Pal K., Heinrich G., Das A., Das C. K.: *Mater. Des*. 2009, **30**, 3839.
23. Zilg C., Thomann R., Mülhaupt R., Finter J.: *Adv. Mater*. 1999, **11**, 49.
24. Ganter M., Gronski W., Reichert P., Mulhaupt R.: *Rubber Chem. Technol*. 2001, **74**, 221.
25. Zhang L. Q., Wang Y., Sui Y., Yu D.: *J. Appl. Polym. Sci*. 2000, **78**, 1873.
26. Ho D. L., Briber R. M., Glinka C. J.: *Chem. Mater*. 2001, **13**, 1923.
27. Cloisite® 30B Typical Physical Properties Bulletin, published by Southern Clay Products.
28. Cloisite® 15A Typical Physical Properties Bulletin, published by Southern Clay Products.
29. Vaia R. A., Ginnelis E. P.: *Macromolecules* 1997, **30**, 8000.
30. Acharya H., Srivastava S. K., Bhowmik A. K.: *Compos. Sci. Technol*. 2007, **67**, 2807.
31. Kumar S., Malas A., Das C. K.: *Polimery* 2012, **57**, 18.
32. Kuila T., Srivastava S. K., Bhowmick A. K., Saxena A. K.: *Compos. Sci. Technol*. 2008, **68**, 3234.
33. Kornnmann X., Lindberg H., Berglund L. A.: *Polymer* 2001, **42**, 1303.
34. Das A., Costa F. R., Wagenknecht U., Heinrich G.: *Eur. Polym. J*. 2008, **44**, 3456.
35. Xie W., Hwu J. M., Jiang G. J., Buthelezi T. M., Pan W. P.: *Polym. Eng. Sci*. 2003, **43**, 214.
36. Zou H., Xu W., Zhang Q., Fu Q.: *J. Appl. Polym. Sci*. 2006, **99**, 1724.
37. Manias E., Kuppa V., Yang D. K., Zax D. B.: *Colloids Surface A* 2001, **187**, 509.
38. Sun Y. Y., Zhang Z. Q., Moon K. Y. S., Wong C. P.: *J. Polym. Sci. Part B: Polym. Phys*. 2004, **42**, 3849.